Published in final edited form as:
Eur J Cell Biol. 2011 May ; 90(5): 376–389. doi:10.1016/j.ejcb.2010.11.016.

AFAP1L1 is a novel adaptor protein of the AFAP family that interacts with cortactin and localizes to invadosomes

Brandi N. Snyder[a,1], **YoungJin Cho**[b,1], **Yong Qian**[c], **James E. Coad**[d], **Jess Cunnick**[b], and **Daniel Flynn**[b,*]

[a] The Mary Babb Randolph Cancer Center and the Department of Cancer Cell Biology, West Virginia University, Morgantown, WV 26505, USA

[b] The Commonwealth Medical College, 501 Madison Ave., Scranton, PA 18510, USA

[c] Health Effects Laboratory Division, Pathology and Physiology Research Branch, National Institute of Occupational Safety and Health, Morgantown, WV 26505, USA

[d] Department of Pathology, West Virginia University, Morgantown, WV, 26505, USA

Abstract

The actin-filament associated protein (AFAP) family of adaptor proteins consists of three members: AFAP1, AFAP1L1, and AFAP1L2/XB130 with AFAP1 being the best described as a cSrc binding partner and actin cross-linking protein. A homology search of AFAP1 recently identified AFAP1L1 which has a similar sequence, domain structure and cellular localization; however, based upon sequence variations, AFAP1L1 is hypothesized to have unique functions that are distinct from AFAP1. While AFAP1 has the ability to bind to the SH3 domain of the nonreceptor tyrosine kinase cSrc via an N-terminal SH3 binding motif, it was unable to bind cortactin. However, the SH3 binding motif of AFAP1L1 was more efficient at interacting with the SH3 domain of cortactin and not cSrc. AFAP1L1 was shown by fluorescence microscopy to decorate actin filaments and move to punctate actin structures and colocalize with cortactin, consistent with localization to invadosomes. Upon overexpression in A7r5 cells, AFAP1L1 had the ability to induce podosome formation and move to podosomes without stimulation. Immunohistochemical analysis of AFAP1L1 in human tissues shows differential expression when contrasted with AFAP1 with localization of AFAP1L1 to unique sites in muscle and the dentate nucleus of the brain where AFAP1 was not detectable. We hypothesize AFAP1L1 may play a similar role to AFAP1 in affecting changes in actin filaments and bridging interactions with binding partners, but we hypothesize that AFAP1L1 may forge unique protein interactions in which AFAP1 is less efficient, and these interactions may allow AFAP1L1 to affect invadosome formation.

Keywords

AFAP1L1; AFAP1; XB130; podosome; cortactin; dentate nucleus; actin

[*]Corresponding author: dflynn@tcmedc.org (D. Flynn).
[1]These authors contributed equally.

INTRODUCTION

Adaptor proteins are non-enzymatic proteins that have the ability to link together different components of cellular signaling complexes through protein-binding motifs. Actin Filament-Associated Protein of 110 kilodaltons (kDa) (AFAP-110/AFAP1) is an adaptor protein with multiple protein binding motifs that is known to function as both an actin binding protein and a cSrc activating protein (Flynn et al., 1993; Qian et al., 2000). The AFAP1 protein binding motifs include two juxtaposed poly-proline rich Src homology 3 (SH3) binding motifs of approximately 10 amino acids with essential prolines at the amino acid number seven and ten positions within the motif (Mayer, 2001), two Src homology 2 (SH2) binding motifs containing a phosphotyrosine residue amino terminal to 1 or 2 negatively charged amino acids followed by a hydrophobic amino acid (Songyang et al., 1993), two pleckstrin homology (PH) domains, a substrate domain (SD) rich in serine and threonine residues that is a substrate for serine/threonine kinases, a helical leucine zipper (Lzip) with a heptad repeat of leucine residues (Kouzarides and Ziff, 1988) for intra- and inter-molecular interactions within itself and other AFAP1 molecules and an actin binding domain (ABD) which is both necessary and sufficient for AFAP1 to interact with actin filaments (Baisden et al., 2001a; Qian et al., 1998; Qian et al., 2000; Qian et al., 2004). AFAP1 is known to bind actin filaments through its carboxy terminal actin filament-binding domain and will multimerize through its leucine zipper, thus enabling it to crosslink actin filaments (Qian et al., 2002). Activation by the serine/threonine kinase PKCα directs AFAP1 to colocalize with cSrc in the perinuclear region of the cell and activate cSrc by binding to the SH3 domain via its N-terminal SH3 binding motif (Gatesman et al., 2004; Walker et al., 2007). Subsequently, cSrc then has the ability to activate downstream cellular signals that affect cell adhesion, invasion and motility (Fincham et al., 1996; Frame and Brunton, 2002).

Upon cSrc binding and activation, AFAP1 and cSrc move to podosomes, adhesion structures found on the ventral membrane of cells which contain an F-actin rich core (Gatesman et al., 2004; Linder and Kopp, 2005). Podosomes also secrete proteases which enable cells to degrade the extracellular matrix, cross tissue barriers and invade. As cSrc activation is known to switch cells from a normal to an invasive phenotype, the activation and movement of cSrc and AFAP1 may be important steps toward promoting cellular changes in adhesion and invasive potential. Also involved in this process is the ability of a cell to assemble, disassemble and remodel its actin cytoskeleton (Yilmaz and Christofori, 2009). As AFAP1 has been shown to affect dynamic changes in actin filament cross-linking (Qian et al., 2004), AFAP1 may also play a role in actin cytoskeleton remodeling in addition to cSrc activation.

AFAP1 represents a family of three proteins that also include Actin Filament Associated Protein 1 Like 1 (AFAP1L1) and Actin Filament Associated Protein 1 Like 2 (AFAP1L2/XB130) so named as a family by the Human Genome Project due to similarity in modular domain structure and amino acid sequence, most notably within their PH domains. There are 250 known PH domain-containing proteins in the human genome and while the amino acid sequences of these PH domains are not well conserved, they are predicted to have a similar structure with a β-barrel with four β strands on one side and three β strands on the other connected by three variable loops connecting β1/β2, β3/β4 and β6/β7 (DiNitto and Lambright, 2006). However, within the AFAP family, the amino acid sequence, as well as structure and placement within the protein, are well conserved between the PH domains, designating them as a related family of proteins. Overall, AFAP1L2/XB130 consists of 818 amino acids and is 35% identical (64% similar) to AFAP1. AFAP1L2/XB130 was also discovered as a cSrc binding protein and contains a shared functional domain structure to AFAP1 including one SH3 motif, three SH2 motifs, 2 PH domains, a coiled-coil region corresponding to the AFAP1 leucine zipper and a sequence similar to the AFAP1 actin binding domain (Xu et al., 2007). However, unlike AFAP1, AFAP1L2/XB130 did not

appear to bind efficiently to actin filaments. AFAP1L2/XB130 does appear to have functions distinct from AFAP1 in that it acts as an intermediary between the RET/PTC kinase and PI-3 kinase pathway in the thyroid (Lodyga et al., 2009).

In this report we characterize the third AFAP family member, AFAP1L1, which also contains a shared domain structure with AFAP1 and AFAP1L2/XB130. Cladistic analysis of the three AFAP family members (data not shown) indicated that AFAP1 and AFAP1L1 are more closely related to each other than to AFAP1L2/XB130, therefore we sought to compare and contrast AFAP1L1 to AFAP1 so as to characterize AFAP1L1 and determine whether it has functions that are shared or distinct relative to AFAP1.

MATERIALS AND METHODS

Cell Culture and Reagents

A7r5, rat aortic smooth muscle cells, were purchased from American Type Culture Collection and grown in Dulbecco's modified Eagle's medium (DMEM, Mediatech) supplemented with 10% fetal bovine serum (FBS, Atlanta Biologicals), 2mM L-Glutamine (Gibco) and penicillin/streptomycin (Mediatech) at 37°C with 5% CO_2. MDA-MB-435, MDA-MB-231, B1A (Dorfleutner et al., 2007), and Cos-1 cells were grown in Dulbecco's modified Eagle's medium (DMEM, Mediatech), 10% fetal bovine serum (FBS, Atlanta Biologicals), 2mM L-Glutamine (Gibco) and penicillin/streptomycin (Mediatech) at 37°C with 5% CO_2. MCF-10A cells were grown in complete Mammary Epithelium Basal Medium supplemented with MEGM SingleQuots (Lonza) and MCF-7 cells were cultured in Modified Eagle's medium containing 10% FBS and 10 μg/ml bovine insulin (Sigma).

Antibodies used for western blotting and immunofluorescence are as follows: anti-AFAP1 (F1) (Flynn et al., 1993), anti-AFAP1 (BD Transduction Labs), anti-cortactin (Millipore), and β–actin (Sigma). Tetramethylrodamine-isothiocyanate (TRITC)-conjugated phalloidin was from Sigma and Alexa Fluor conjugated phalloidin and secondary antibodies were from Invitrogen. The antibody against AFAP1L1, 1L1-CT, was generated by ProSci Incorporated. Rabbits were immunized with AFAP1L1 peptide corresponding to amino acids 714–727. 1L1-CT antibody was affinity-purified by affinity absorption against the AFAP1L1 peptide attached to an Ultralink Iodoacetyl column (Pierce) according to manufacturer's protocol. Two additional antibodies against AFAP1L1, Ab1 and Ab2, targeting either the C terminus (amino acid 525–659) or the N terminus (amino acids 21–159) of 1L1, respectively, were from Sigma.

Constructs

The *afap1l1* cDNA sequence was purchased in two vectors from OpenBioSource. The coding sequence for AFAP1L1 amino acids 1 through 340 was identified in a pCMV-SPORT6 vector. The coding sequence for AFAP1L1 amino acids 273 through 768 was identified in a pINCY vector. A BstYI restriction site, GATCC, in the overlap region was mutated to a BglII restriction site, GATCT, to create a unique restriction site using the Stratagene QuikChange Site-Directed Mutagenesis Kit according to manufacturer's protocol. AFAP1L1 N-terminal coding sequence was subcloned into pBluescript II KS (Stratagene) using HindIII and an engineered EcoRI restriction site. AFAP1L1 C-terminal coding sequence was subcloned into pBluescript II KS using engineered HindIII and EcoRI restriction sites. Full length AFAP1L1 was created by restriction digest of pBluescript containing each AFAP1L1 coding sequence with the unique BglII site in the overlap region and a unique Sca1 site found in the vector followed by fusion of the two halves of pBluescript. The AFAP1L1 full length sequence was confirmed by DNA sequencing.

Full length AFAP1L1 was subcloned into pEGFP (Clonetech) using HindIII and EcoRI. Full length AFAP1L1 was subcloned from pEGFP into pcDNA3.1(+) hygro (Invitrogen) using HindIII and Kpn1. GFP-AFAP1 was previously described by (Qian et al., 2000).

Transfection

For antibody characterization and GST pull down overexpression studies respectively, Cos-1 and 293T cells were transiently transfected with 5μg of either GFP-AFAP1 or GFP-AFAP1L1 using Lipofectamine and Plus reagent according to manufacturer's protocol. For confocal overexpression studies, mouse embryo fibroblasts (MEF) were transfected with 5μg of either GFP-AFAP1L1 or untagged AFAP1L1 (in pcDNA3.1) using Lipofectamine and Plus reagent. To determine endogenous AFAP1L1 localization to invadopodia, MDA-MB-435 cells were transfected with cSrc527F plasmid using Lipofectamine and Plus reagent (Invitrogen) according to the manufacturer's instructions. A7r5 cells were transfected with GFP-AFAP1 or GFP-AFAP1L1 in increasing amounts from 0.1 μg to 1.0 μg using Lipofectamine and Plus reagent per well of a 6 well plate. Total DNA concentration for dose response transfections was kept constant using an empty pcDNA3.1 vector to keep the total DNA transfected at 1.0 μg to maintain equal transfection efficiency.

Immmunoblotting

Cos-1 cells transiently expressing GFP-AFAP1 or GFP-AFAP1L1 were lysed in 2X SDS buffer (125mM Tris-HCl pH6.8, 20% glycerol, 4% SDS). Cell lines MCF-10A, MCF-7, MDA-MB-231, MDA-MB-435, B1A, and Cos-1 were lysed in 2X SDS buffer. Protein concentration was determined using a BCA Protein Assay Kit (Pierce) according to manufacturer's protocol. 50μg of total lysate was resolved by 8% SDS-PAGE. Proteins were transferred to polyvinylidene fluoride (PVDF) membrane (Immobilon-P, Millipore) using semi-dry electroblotting. Proteins were detected by incubation with either anti-1L1-CT (ProSci) 1:250, anti-1L1-Ab1 (Sigma) 1:1000, anti-1L1-Ab2 (Sigma) 1:500, anti-AFAP1 (BD Transduction Labs) 1:10000, anti-AFAP1 (F1) 1:20000, anti-GFP (Zymed) 1:1000 or anti-β-actin (Sigma) 1:10000 in 5% powdered milk (TBS, 0.05% Tween-20) followed by incubation with 1:3000 dilution of donkey anti-mouse or donkey anti-rabbit horseradish peroxidase conjugated antibodies (GE Healthcare Bio-Sciences). Chemiluminescence was visualized with Pierce ECL Western Blotting Substrate.

Immunofluorescence

MDA-MB-435, MEF and A7r5 cells were grown on fibronectin-coated coverslips (50μg/ml) overnight at 37°C. For GFP-AFAP1L1 overexpression and overexpressed untagged AFAP1L1, MEF and A7r5 cells were fixed with 3.7% formaldehyde, permeabilized with 0.2% triton X-100 and incubated with or without anti-cortactin antibody (1:200). Actin filaments were decorated with TRITC-phalloidin (1:600) or Alexa Flour conjugated phalloidin (1:100). For endogenous AFAP1L1 staining, MDA-MB-435 were fixed and permeabilized in 3.7% formaldehyde containing 0.1% triton X-100, incubated with Alexa Flour conjugated phalloidin (1:100) in 3% BSA, and then stained with anti-AFAP1L1 antibodies Ab1 or Ab2 (Sigma, 2 μg/ml) and anti-cortactin antibodies. Fluorescence conjugated secondary antibodies (Invitrogen) were used at a 1:200 dilution. Coverslips were mounted on slides using Prolong Gold (Invitrogen) and imaged with a Zeiss LSM 150 microscope or Nikon eclipse Ti inverted epi-fluorescence microscope. Podosomes were confirmed by anti-cortactin localization along the basolateral membrane via confocal microscopy (0.5 μm scanning thickness). Images were further processed with Zeiss LSM Image Browser (Zeiss), CorelDRAW12, Nikon NIS element software (Nikon) and Adobe Photoshop.

Immunoprecipitation

Cos-1 cells were lysed in RIPA buffer (50mM Tris pH7.5, 150mM NaCl, 2mM EDTA, 1% Igepal, 0.25% sodium deoxycholate, 10mM β-glycerol, 1mM sodium vanadate, 5μg/μl aprotinin, 5μg/μl leupeptin, 1mM PMSF). 1 mg of Cos-1 lysate was used for each control IgG, anti-1L1-CT and AFAP1 (F1) pull down. Lysates were pre-cleared with agarose A beads for one hour. The precleared lysates were incubated on ice for one hour with 2μg IgG, 1L1-CT or F1 antibodies, and then 50% slurry agarose A beads were added and incubated for one hour. Proteins were eluted from beads using 2X Laemmli sample buffer (LSB) with 200mM dithiothreitol (DTT), separated by 8% SDS-PAGE and processed for western blot analysis. 293T cells were transfected with human cortactin cDNA with either EGFP AFAP1 or AFAP1L1 construct using Polyfect (Qiagen) according to the manufacturer's specification. Forty-eight hours post transfection, cells were lysed in RIPA buffer and 2 mg of cell lysates were used for immunoprecipitation with either GFP antibodies (Polyclonal Av antibodies, Clonetech) or cortactin antibodies (clone 4F11, Millipore) as described above.

Immunohistochemical methods

Immunohistochemistry was performed on de-identified human brain, breast and colon tissue slices obtained from the West Virginia University Department of Pathology Tissue Bank. Tissues were paraffin-embedded and cut into 5 μm-thick sections and mounted on positive-charge coated slides. Tissue sections were dried overnight in a 45°C oven, deparaffinized, rehydrated, and subjected to heat-induced epitope retrieval for two hours in 1 mM citrate buffer (pH 6.00) in an 80° C water bath. Endogenous peroxide activity was blocked with 3% hydrogen peroxide and was followed by treatment with a serum-free protein blocker to block non-specific binding. Following each step of the immunoreaction except the protein blocker, sections were rinsed in Tris-buffered saline with Tween-20. Tissues were incubated for two hours with either anti-AFAP1 antibody (F1) at a dilution of 1:50 or with anti-1L1-CT diluted 1:50 in 10% normal horse serum. Negative controls (i.e., preimmune serum or normal rabbit IgG) were incubated in 10% normal horse serum. Sections were incubated with biotinylated-linked secondary antibody, followed by treatment with streptavidin peroxidase and stained with diaminobenzidine substrate-chromogen solution. Counterstaining was performed with hematoxylin, followed by a water rinse and bluing solution. Tissues were then dehydrated and mounted with coverslips

Affinity precipitation with GST fusion proteins

293T cells transiently expressing GFP-AFAP1 or GFP-AFAP1L1 were lysed in Modified RIPA buffer (50 mM Tris pH 7.5, 150 mM NaCl, 2mM EDTA, 1% Igepal, 0.25% sodium deoxycholate, 10 mM β-glycerol, 1 mM sodium vanadate, 5μg/μl aprotinin, 5μg/μl leupeptin and 1μM PMSF). GFP-AFAP1 and GFP-AFAP1L1 lysates were pre-cleared using 50 μg of GST protein bound to Glutathione Sepharose 4B coated beads (GE Healthcare) and 1mg of each pre-cleared lysate was incubated at 4°C for 1 hour with either 50 μg control GST, 50 μg GST-Src SH3 domain or 50 μg GST-cortactin SH3 domain bound to GST beads. Proteins were eluted from beads by boiling for 5 minutes in 2X Laemmli sample buffer with 200mM DTT and further processed with PAGE and western blot analysis. Western blot results were examined with ImageJ densitometry analysis so as to provide a ratio between the amount of AFAP1 and AFAP1L1 pulled down with each GST or GST fusion protein.

RESULTS

Identification of AFAP1L1

AFAP1L1 was discovered during a homology search of the human genome using sequences of the AFAP1 PH domains and was subsequently referred to as the third member of the

AFAP family by the Human Genome Project. The *afap1l1* gene is located on chromosome 5q33.1 and consists of 19 exons that are predicted to encode 768 amino acids in the open reading frame (Figure 1). All AFAP family members contain at least one predicted N-terminal SH3 binding motif, at least one predicted N-terminal SH2 binding motif, two PH domains separated by a region rich in serine and threonine residues and a C-terminal SH2 binding motif (Figure 2A). One major difference is found in the C-terminus where AFAP1 and AFAP1L1 contain a leucine zipper and actin binding domain while AFAP1L2/XB130 contains a related coiled-coil in this respective region (Figure 2B) (Baisden et al., 2001b; Xu et al., 2007).

There appear to be differences in the SH3 binding motif of AFAP1L1 compared to AFAP1. AFAP1 contains two juxtaposed SH3 binding motifs, PPQMPLPEIP and PPDSGPPPLP, beginning at amino acids 65 and 76 respectively (Guappone and Flynn, 1997). AFAP1 will bind cSrc using the N-terminal P^{71}EIP of the first SH3 binding motif (Guappone and Flynn, 1997), while AFAP1L2/XB130 has been reported to also bind cSrc through its SH3 binding motif, identified as PDLPPPKMIP (Xu et al., 2007). However, the AFAP1L1 coding sequence contains only one predicted SH3 binding motif in its amino terminus, DLPPPLPNKP, which is not consistent with a consensus cSrc SH3 binding motif but may have the ability to bind to other SH3 domains.

AFAP1 contains two SH2 binding motifs that interact with cSrc, YYEEA in the N-terminal portion of the protein and YDYI in the C-terminal portion, which are both sites for tyrosine phosphorylation (Guappone et al., 1998). AFAP1L1 shares 100% sequence identity with both AFAP1 and AFAP1L2/XB130 in its predicted N-terminal SH2 binding motif, YYEEA, and is highly similar in its C-terminal SH2 binding motif YDYV (Guappone et al., 1998; Xu et al., 2007). Thus, these may be potential sites for tyrosine phosphorylation.

The N-terminal and C-terminal PH domains of the AFAP family share sequence similarity and, thus, can be predicted to share structural similarity. The amino acid sequence intervening between the PH domains of AFAP1 (substrate domain, SD, Figure 2B) is rich in serine and threonine residues (Qian et al., 2002). $Serine^{277}$ in AFAP1 is a known target of phosphorylation by PKCα and plays a role in the ability of AFAP1 to regulate podosome formation and lifespan (Dorfleutner et al., 2008). AFAP1L1 and AFAP1L2/XB130 also have multiple serine and threonine residues in the sequence flanked by their PH domains, although these sequences have not been confirmed to be phosphorylated by serine/threonine protein kinases.

The leucine zipper of AFAP1 is essential for intra-molecular regulation of AFAP1 and interaction with other AFAP1 molecules and is directly adjacent to the actin binding domain (Qian et al., 2004). AFAP1L1 contains a similar sequence that may have the ability to act as a leucine zipper or coiled-coil motif as well as a putative actin binding domain which is similar to the known actin filament binding domain found in AFAP1 (Qian et al., 2000). AFAP1L2/XB130 contains a coiled-coil motif in its C-terminus and a sequence that is similar to the AFAP1 actin binding domain, but AFAP1L2/XB130 has not been demonstrated to bind actin filaments (Xu et al., 2007). An amino acid sequence alignment of the three family members found that AFAP1 and AFAP1L1 overall share 44% identity and 71% similarity while AFAP1L1 and AFAP1L2/XB130 share 31% identity and 61% similarity and their sequences predict conserved functional domains within the proteins (Figure 2B).

A novel antibody is specific for AFAP1L1

A rabbit polyclonal antibody was generated against the carboxy terminal amino acids 714–727 of human AFAP1L1. We refer to this antibody as 1L1-CT. We also utilized two

commercially available AFAP1L1 antibodies, called Ab1 (epitope defined as amino acids 525–659) and Ab2 (epitope defined as amino acids 21–159). The ability of these antibodies to detect AFAP1L1 was studied using lysates of human breast lines MCF-10A, MCF-7, MDA-MB-231, B1A (a variant of MDA-MB-231 cells that had AFAP1 knocked down using shRNA (Dorfleutner et al., 2007)), MDA-MB-435 as well as monkey kidney cell line Cos-1. All three AFAP1L1 antibodies detected a distinct protein band by western blot analysis with a M_r of 115 kDa (Figure 3A, result from Ab2 as a representative example) with MDA-MB-435 having the highest endogenous expression levels of AFAP1L1 among the tested cell lines. The M_r of AFAP1L1 was further confirmed by siRNA knockdown against AFAP1L1 (data not shown). The expression pattern of AFAP1L1 across breast cancer cell lines was further confirmed in messenger RNA levels through quantitative RT-PCR analysis (data not shown). To test the ability of the 1L1-CT antibody to immunoprecipitate endogenous AFAP1L1, Cos-1 cells were lysed and 1mg of lysate (1μg/μl) was incubated with either 5μg 1L1-CT, 5μg AFAP1 antibody F1 or 5μg control rabbit IgG and the immunoprecipitate resolved by SDS-PAGE (Figure 3B). Upon western blot analysis with 1L1-CT, it was apparent that the 1L1-CT antibody specifically immunoprecipitated a protein with a M_r of 115kDa, consistent with the predicted M_r for AFAP1L1 (Figure 3B, left panel, middle lane); while the AFAP1 antibody F1 did not immunoprecipitate a protein of this M_r (Figure 3B, left panel, right lane) that could be detected by the 1L1-CT antibody. To test the specificity of F1 antibody for endogenous AFAP1, Cos-1 cells were lysed and 1.5mg (1μg/μl) of lysate was incubated with rabbit IgG, F1 or 1L1-CT. F1 antibody specifically immunoprecipitated the expected AFAP1 protein with an M_r of 110 kDa (Figure 3B, right panel, right lane) and did not immunoprecipitate AFAP1L1 (Figure 3B, right panel, middle lane), indicating that these two antibodies are specific for endogenous protein. To determine if 1L1-CT and F1 antibodies can specifically recognize overexpressed protein, plasmids encoding GFP-AFAP1L1 and GFP-AFAP1 were transfected into Cos-1 cells. Western blot analysis of these cells (Figure 3C) showed that 1L1-CT antibody detected overexpressed GFP-AFAP1L1 but not overexpressed GFP-AFAP1 (Figure 3C, left panel). AFAP1 antibody F1 detected GFP-AFAP1 but not GFP-AFAP1L1 (Figure 3C, middle panel). These data indicate that the AFAP1L1 antibody 1L1-CT and AFAP1 antibody F1 have specificity for AFAP1L1 and AFAP1, respectively. These data also indicated that 1L1-CT antibody is specific to the AFAP1L1 of human and monkey species. 1L1-CT antibody did not recognize any distinct band in murine cell lysates (data not shown), because the epitope is not conserved in murine AFAP1L1 (Figure 3D). Sigma antibodies Ab1 and Ab2 also failed to recognize AFAP1L1 in murine cell lysates. An alignment of the peptide sequence used to create 1L1-CT against the amino acid sequence of human, chimpanzee, mouse and rat AFAP1L1 was shown to illustrate the similarity of the 1L1-CT binding site across species (Figure 3D).

Immunohistochemical analysis of AFAP1L1

The ability of the 1L1-CT antibody to specifically recognize endogenous AFAP1L1 in its native conformation by immunoprecipitation and to recognize AFAP1L1 by immunofluorescence (Supplemental Figure 1) demonstrated its usefulness for immunohistochemistry. To determine the tissue localization of AFAP1L1, immunohistochemistry was performed on human breast, colon and brain tissues using 1L1-CT antibody (Figure 4). AFAP1 or AFAP1L1 tissue localizations were compared using sequential sections of tissue immunolabeled with F1 or 1L1-CT antibodies, respectively, in order to contrast expression patterns. In the breast, AFAP1 was found to strongly associate with the ductal cells and also the breast microvasculature (Figure 4A panels a, c and e). AFAP1L1 was found in the contractile myoepithelial cell layer which surrounds the breast ducts and in the microvasculature (Figure 4A panels b, d and f), similar to AFAP1. In the colon (Figure 4B), AFAP1 was found in the epithelial mucous membrane as well as in the

colonic crypts (Figure 4B panels a and g) which aid in mucous production and production of new epithelial cells for the intestinal surface (Sherwood, 2003). AFAP1L1 was also found in the mucous membrane and colonic crypts (Figure 4B panels b and h). Both AFAP1 and AFAP1L1 are found in the microvasculature (Figure 4B panels a–d) while AFAP1 can also be found in nerves that pass through the lamina propria (Figure 4B panel g). The lamina propria lies directly beneath the epithelial cell layer and consists of connective tissue, blood vessels, nerve fibers and lymphatic ducts (Widmaier, 2003). The muscularis, layers of smooth muscle which provide movement of the colon, expresses both AFAP1 and AFAP1L1 (Figure 4B panels c–f) while AFAP1 is solely found in Auberbach's plexus (Figure 4B panel e), the nerves that innervate the muscle of the gut (Sherwood, 2003). While AFAP1 and AFAP1L1 have overlapping localization in human breast and colon tissue, human brain showed examples of differential expression patterns for these two proteins (Figure 4C). The cerebellum is located at the base of the skull and is an important part of the motor system. Divided into three layers, the cerebellar cortex is composed of a granular cell layer consisting of small granule cells which receive input from mossy fibers and extend into the molecular layer, the outermost portion of the cerebellar cortex which houses stellate and basket cells. Purkinje cells are large neurons acting as the sole output of motor coordination from the cerebellar cortex and are found in a single layer between the molecular and granular layers (Squire, 2008). AFAP1 is found in the microvasculature of the brain, in the molecular layer and meningeal vessels and to a slight level around the granule cells of the granular layer (Figure 4C panels a, c, e and g). AFAP1L1 is again found in low levels in the microvasculature of the brain but is localized around the Purkinje neurons and the granule cells of the granular layer (Figure 4C panels b, d, f and h). This immunolabeling is not inside of either the Purkinje neurons or the granule cell bodies but instead extends away from the cell body. Although the source of this immunolabeling is unknown, mossy fibers and climbing fibers extend into the granule cell layer and Purkinje cell layer respectively, synapsing onto granule and Purkinje cells (Squire, 2008). This may provide the source of immunolabeling for AFAP1L1 away from the granule and Purkinje cell body. Outside of the cerebellar cortex, AFAP1 and AFAP1L1 are both found in glial cells (Figure 4C panels o–p) but have a differential expression pattern in the dentate nucleus (Figure 4Ck–n), one of four deep cerebellar nuclei responsible for voluntary movements of the extremities (Squire, 2008). Again, AFAP1L1 is highly expressed away from the cell bodies within the dentate nucleus, while AFAP1 was not detected in this structure. Relative intensities of immunohistochemical signal for AFAP1 and AFAP1L1 are presented in Table 1.

AFAP1L1 subcellular localization

AFAP1 is known to bind actin filaments, move to actin rich structures called podosomes upon stimulation with the phorbol ester PDBu and also to be localized in podosome-like structures termed invadopodia in MDA-MB-231 cells, while AFAP1L2/XB130 is not known to bind actin filaments (Flynn et al., 1993; Gatesman et al., 2004; Xu et al., 2007). Thus, we sought to determine if AFAP1L1 had the potential to be localized with actin filaments and podosomes, similar to AFAP1 (Gatesman et al., 2004). For this analysis, we used the rat-derived A7r5 cell line, a well established cell model system for podosome formation (Hai et al., 2002). Overexpression of GFP-AFAP1L1 alone in A7r5 cells produced two distinct phenotypes (Figure 5A). GFP-AFAP1L1 expressing cells either have GFP-AFAP1L1 decorating actin stress fibers while cortactin is found in the cytoplasm and around the cell periphery (Figure 5A panels a–d) or both GFP-AFAP1L1 and cortactin colocalizing in punctate actin dots along the ventral membrane (Figure 5A and Supplemental Figure 2). The adaptor protein cortactin was used as a marker for podosome formation. Podosome formation was observed either around the cell periphery (5A panels e–h) or scattered across the ventral membrane (5A panels i–l). Thus, AFAP1L1 decorates actin

stress fibers and co-localizes with cortactin in podosomes. Overexpression of AFAP1L1 induced the formation of podosomes in a small percentage of cells. Next, we utilized MDA-MB-435 cells to determine the subcellular localization of endogenous AFAP1L1 based on the high level of expression of AFAP1L1 in this cell line. Immunolabeling of MDA-MB-435 with Sigma Ab2 (Figure 5B, panel a–c) and Ab1 (data not shown) showed a population of AFAP1L1 decorating actin stress filaments while the rest of AFAP1L1 was detected diffusely across the cytoplasm. A similar pattern of expression was observed for the 1L1-CT antibody in MEF cells overexpressing untagged AFAP1L1 (Supplemental Figure 1). To determine whether endogenous AFAP1L1 could co-localize to invadopodia, we transiently transfected a constitutively active Src construct (Src527F) into MDA-MB-435 to induce invadopodia, podosome-like structures found in cancer cells. The overexpression of Src527F induced punctate actin- and cortactin-rich structures in these cells (Figure 5C, b–c, f–g) accompanied by the loss of stress filaments, which were consistent with the appearance of typical invadopodia. The immunolabeling of endogenous AFAP1L1 (Figure 5C, a) showed discernable association with invadopodia, co-localizing with cortactin and actin (Figure 5C, a–d, marked with white arrow as an example of colocalization). These data indicate that AFAP1L1, like AFAP1, is associated with actin stress filaments and localizes to invadosomes (the collective term for podosomes and invadopodia) at both overexpressed and endogenous levels (also see Supplemental Figure 3) (Linder, 2009; Saltel et al., 2010).

Quantification of podosome formation in A7r5 expressing AFAP1 or AFAP1L1

In a previous study of AFAP1, expression of GFP-AFAP1 was sufficient to induce podosomes in a portion of the A7r5 cells in which it was expressed (Dorfleutner et al., 2008). Therefore, we sought to compare the potency of the GFP-AFAP1 and GFP-AFAP1L1 constructs to induce podosomes using a dose response analysis. A7r5 cells were transfected with equal amounts of total plasmid cDNA containing the indicated amount of GFP-AFAP1 or GFP-AFAP1L1 plasmid (Figure 6). Transfection of equal amounts of plasmid (combination of empty vector and GFP-AFAP) ensured that transfection efficiencies were identical for each dose of plasmid. Forty eight hours after transfection, the cells expressing either GFP-AFAP1 or GFP-AFAP1L1 were assessed for podosome formation. Reduction of plasmid DNA resulted in a corresponding reduction of GFP-AFAP1 and GFP-AFAP1L1 expression (Figure 6A). The reduction of expression was also reflected in a reduction in the percent of cells exhibiting podosomes (Figure 6B). When 1μg and 0.35 μg of plasmid DNA was used, the percentage of GFP-AFAP1 expressing cells exhibiting podosomes dropped from 11.4% to 7.1% while in GFPAFAP1L1 expressers the change was more modest, 9.2% to 8.0%. At 0.1 μg of DNA the number of podosome cells appeared to increase. This increase resulted from the variability in expression levels among cells and the dimness of the low expressers which made these cells difficult to detect by immunofluorescence. Overall, this experiment demonstrated that under identical conditions of transfection, expression, processing and immunofluorescence analysis, expression of GFP-AFAP1 and GFP-AFAP1L1 induce podosome formation in A7r5 cells.

Interaction of AFAP1L1 and cortactin

To determine if AFAP1L1 might have a differential ability to interact with proteins relative to AFAP1, we screened SH3 domains from various proteins for the binding to AFAP1L1. A Panomics array screening of SH3 domains showed that the SH3 domain of cortactin and the SH3 binding motif of AFAP1L1 had a strong potential to interact (data not shown). To confirm these screening results, GST fusion proteins containing the cortactin SH3 domain and the Src SH3 domain were incubated with 1mg of cell lysate containing either overexpressed GFP-AFAP1L1 or GFP-AFAP1. As expected from the known binding of AFAP1 to Src, AFAP1 showed a strong interaction with the Src SH3 domain with a 14-fold increase in the ratio of AFAP1 pulled down by GST-Src SH3 as compared to GST control

while precipitation by the cortactin SH3 domain was undetectable (Figure 7A). However, AFAP1L1 was more efficiently precipitated by GST-SH3-cortactin than GST-SH3-Src with an approximately 9-fold increase in the ratio of AFAP1L1 pulled down by GST-cortactin SH3 compared to GST control (Figure 7B). These data indicate that the SH3 binding motifs of AFAP1 and AFAP1L1 have the ability to interact with different affinities toward different SH3 binding partners. To further examine the potential binding of AFAP1L1 with cortactin, we transiently overexpressed either GFP-AFAP1 or GFP-AFAP1L1 with cortactin in 293T cells. GFP-AFAP1L1 co-immunoprecipitated with cortactin (Figure 7C, upper panel) more efficiently than did GFP-AFAP1 (the amounts of immunoprecipitated GFP proteins were relatively equal Figure 7C, lower panel). Conversely, cortactin specifically co-immunoprecipitated GFP-AFAP1L1, but not GFP-AFAP1 (Figure 7D, upper panel). These data suggest that cortactin can form a complex with AFAP1L1, but is either unable to form a complex with AFAP1 or its ability to bind in a complex with AFAP1 is below detection limits. This interaction is hypothesized to occur through SH3 interactions based on our affinity precipitations with the SH3 domains and suggests a unique function for AFAP1L1 that is distinct from AFAP1.

DISCUSSION

AFAP family amino acid sequence

AFAP1 is a well-studied cSrc binding partner and actin filament cross-linking protein that is the prototype member of what is predicted to be a family of three proteins which also includes AFAP1L1 and AFAP1L2/XB130. There are no published reports on AFAP1L1 and the goal of this study was to analyze some of the similarities and differences between AFAP1 and AFAP1L1 in order to understand what functions AFAP1L1 may have relative to AFAP1. The AFAP family consists of three family members that share similarity in protein binding motifs including both PH domains. Analysis of the overall amino acid structure of previously described AFAP1 and newly presented AFAP1L1 show 44% identity and 71% similarity between the two proteins. AFAP1 contains two juxtaposed SH3 binding motifs in its N-terminus, PPQMPLPEIP and PPDSGPPPLP, of which the first is necessary for efficient cSrc binding. Mutation of a necessary proline, Pro^{71}, to an alanine, Ala^{71}, in the AFAP1 SH3 binding motif prevented cSrc binding (Guappone and Flynn, 1997). While AFAP1L1 only contains one putative SH3 binding motif, DLPPPLPNKP, this sequence is not consistent with the conserved consensus cSrc SH3 binding motif. Rather, the AFAP1L1 SH3 binding motif more closely resembles that of a cortactin SH3 domain binding site, which preferentially binds a +PPΨPXKPXWL motif where + is a basic residue, Ψ is an aliphatic residue, and X is any amino acid (Sparks et al., 1996).

In addition to the SH3 binding motif, cSrc also has the ability to phosphorylate and bind two SH2 binding motifs in AFAP1. In AFAP1, an N-terminal YYEEA sequence adjacent to the SH3 binding motifs and a C-terminal YDYI sequence have been shown to be phosphorylated by cSrc (Guappone et al., 1998). AFAP1L1 contains the conserved YYEEA sequence in its N-terminus adjacent to the SH3 binding motif and a similar YDYV sequence in its C-terminus. Although we did not analyze AFAP1L1 as a possible target for phosphorylation by tyrosine kinases, these similar SH2 binding motifs may be potential targets for tyrosine phosphorylation. A ScanSite motif scan comparison between AFAP1 and AFAP1L1 predicts these sites for tyrosine phosphorylation and also predicts similar sites for serine/threonine phosphorylation as well (data not shown). The amino acid sequences between the PH1 and PH2 domains of AFAP1 and AFAP1L1 are rich in serine and threonine residues that are predicted to be sites of serine and threonine phosphorylation. In particular, AFAP1 is known to be phosphorylated on serine 277 by PKCα and this phosphorylation is important for podosome turnover (Dorfleutner et al., 2008). Although we

have not validated AFAP1L1 as a PKC substrate, AFAP1L1 also contains a similar PKCα phosphorylation site.

The conservation of domain structure, overall sequence similarity and high similarity of sequence between the two PH domains indicates that AFAP1, AFAP1L1 and AFAP1L2/XB130 are members of a family of proteins, referred to here and in genome databases as the AFAP family. The amino terminal PH1 domain of AFAP1 has been known to function in intra-molecular regulation of AFAP1 (Qian et al., 2004). In addition, the PH1 domain is a binding partner for PKCα and phospholipids (Cunnick and Flynn, manuscript in preparation) (Qian et al., 2002).

The actin binding domain within AFAP1 is necessary and sufficient for the binding of AFAP1 to actin filaments (Qian et al., 2000). Comparison of the AFAP1 actin binding domain sequence to the corresponding sequence in AFAP1L1 does not indicate a high level of similarity although our data indicates that AFAP1L1 also has the ability to associate with actin filaments. We predict that the sequences within the C-terminus of AFAP1L1 that are similar to the known actin filament binding domain in AFAP1 may promote actin filament association, however, as the binding affinity of AFAP1 for actin is relatively low, we predict that the putative actin binding domain of AFAP1L1 may have a lower affinity for actin. Studies are underway to determine the mechanism of actin filament binding and if the leucine zipper/coiled-coil motif adjacent to the putative actin filament binding domain can regulate self-association and actin filament cross-linking, similar to AFAP1 (Qian et al., 2004).

AFAP1L1 western blot analysis

AFAP1L1 can be found in human breast and breast cancer cell lines, as well as the Cos-1 monkey cell line. The predicted molecular weight of AFAP1L1 is 85kDa, but it is detected as a single protein band by western blot analysis with a M_r of 115 kDa, Similarly, AFAP1 has a molecular weight of 82 kDa but is detected on western blot as a 110 kDa protein.. For AFAP1, it was hypothesized that the difference in molecular weight and M_r might be due to overall charge and the shape of the protein, which may also apply to AFAP1L1. The AFAP1L1 specific antibodies, 1L1-CT, Ab1 and Ab2 antibodies (latter two from Sigma), have the ability to specifically detect AFAP1L1 but not AFAP1 by western blot. In our hands, all three antibodies could detect AFAP1L1 by immunoprecipitation, immunofluorescence and western blot; however, the 1L1-CT antibody was determined to be less efficient in detecting denatured AFAP1L1 by western blot, indicating that this antibody may preferentially recognize a conformational epitope and be less efficient in detecting denatured AFAP1L1, relative to Ab1 and Ab2, which appear to detect denatured AFAP1L1 efficiently. Conversely, the anti-AFAP1 antibody F1 is able to specifically immunoprecipitate AFAP1 but does not immunoprecipitate AFAP1L1.

AFAP1L1 tissue expression pattern

AFAP1 and AFAP1L1 have similar distribution in breast and colon tissue with the exception that AFAP1 can be found in the nerves that innervate the gut while AFAP1L1 was not detected there. While immunolabeling of the brain shows similarities between AFAP1 and AFAP1L1 in the granule cell layer and glial cells, differences occur in the brain where AFAP1L1 is found in the Purkinje cell layer and the dentate nucleus, while AFAP1 was not detected here. The dentate nucleus is known to be involved in motor coordination; alterations in the neuronal composition of signaling to and from the dentate have been implicated in diseases with motor dysfunction such as Alzheimer's disease, autism spectrum disorders and Pick's disease (Braak et al., 1999; Fukutani et al., 1999; Lotspeich and Ciaranello, 1993). Consistent immunolabeling of AFAP1L1 between the granule cell layer,

Purkinje layer and dentate nucleus indicates that the AFAP1L1 immunohistochemical signal is not in the cell bodies of the granule cells, Purkinje neurons or cells of the dentate nucleus, but is instead found extending away from the cell body. Thus, we hypothesize that AFAP1L1 may be playing a role in either the axon terminals of afferent neurons or the dendritic spines of efferent neurons in these areas, both of which have a dynamic actin cytoskeleton and are rich in proteins involved in cytoskeletal remodeling, such as cortactin (Hering and Sheng, 2003). As we see the most marked difference between AFAP1 and AFAP1L1 expression in the dentate nucleus, we speculate that AFAP1L1 may play a role in the association of proteins involving signaling to or from the dentate nucleus. Notably, podosomes have recently been shown to be involved in maturation of the neuromuscular junction and a similar mechanism may be involved in neuron-neuron interactions (Proszynski et al., 2009).

AFAP1L1 subcellular localization and podosome formation

GFP-AFAP1L1 and endogenous AFAP1L1 colocalized with actin filaments and invadosomes similar to the subcellular localization pattern of AFAP1. Overexpression of GFP-AFAP1L1 induced podosome formation in the absence of extracellular signals (e.g., phorbol ester). A direct comparison of the ability of GFP-AFAP1 and GFP-AFAP1L1 to induce podosomes demonstrated that both proteins had similar capacities to induce these structures. Thus, like AFAP1, AFAP1L1 may have the ability to interact with proteins involved in podosome formation such as f-actin, cSrc or possibly cortactin. A panomics array of various SH3 domains was scanned for the ability to bind the AFAP1L1 SH3 binding motif, and these data indicated that the AFAP1L1 SH3 binding motif and the cortactin SH3 domain showed the strongest interaction among those SH3 domains surveyed (data not shown). GST fusion proteins containing either the cortactin SH3 domain or Src SH3 domain show that AFAP1 interacted with GST-Src SH3 much better than with GST-cortactin SH3. However, with AFAP1L1 the reverse was true. AFAP1L1 interacted with GST-cortactin-SH3 better than GST-Src SH3. These data indicate that the SH3 binding motifs of AFAP1 and AFAP1L1 likely have different affinities for different SH3 binding partners. The co-immunoprecipitation of cortactin with full length AFAP1L1 and not with AFAP1 further supports the possibility of differential characteristics of these two proteins and also suggests the interaction of AFAP1L1 with cortactin as a possible mechanism of AFAP1L1 localization to invadosomes. Investigations are underway to determine if the SH3 binding motif of AFAP1L1 mediates the binding of AFAP1L1 to cortactin and to determine the functional relevance of this interaction.

Conclusion

The goal of this study was to characterize the AFAP family member AFAP1L1 and to determine if it had functions common and distinct to AFAP1. Our data indicate that AFAP1L1 has strong similarity and conservation of domain structure with AFAP1. Also similar to AFAP1, it has an ability to associate with actin filaments, can be found in actin-rich structures such as invadosomes, and is capable of independently inducing podosomes upon overexpression. AFAP1L1 shares expression patterns with AFAP1 in several tissues. However, AFAP1L1 did display some unique properties. For example, unlike AFAP1, AFAP1L1 was found in the dentate nucleus and its expression appeared to occur along neuronal processes. Interestingly, it is in these processes that podosomes are hypothesized to be associated with synaptic connections (Proszynski et al., 2009), and these same connections in the dentate nucleus contain cortactin binding proteins (Hering and Sheng, 2003). As podosomes play a role in enabling cells to traverse and cross tissue barriers, we hypothesize that AFAP1L1 may play a unique role in the innervation of the dentate nucleus. Although it may have a weak affinity, AFAP1L1 is not predicted to be a strong binding partner for cSrc through SH3 interactions; however, it does interact with cortactin. As a

potential binding partner for actin filaments and cortactin, AFAP1L1 may associate with podosomes via interactions with these proteins and regulate podosome formation in cells, including neurons within the dentate nucleus.

Supplementary Material

Refer to Web version on PubMed Central for supplementary material.

Acknowledgments

We thank the lab of Scott Weed for the GST cortactin SH3 construct and the full length cortactin construct. We thank the lab of Steven M. Frisch for MCF-10A cells. We also thank Albert Berrebi for advice and consultation on evaluation of the dentate nucleus. This work was supported by the NIH (R01CA60731).

References

Baisden JM, Gatesman AS, Cherezova L, Jiang BH, Flynn DC. The intrinsic ability of AFAP-110 to alter actin filament integrity is linked with its ability to also activate cellular tyrosine kinases. Oncogene. 2001a; 20:6607–6616. [PubMed: 11641786]

Baisden JM, Qian Y, Zot HM, Flynn DC. The actin filament-associated protein AFAP-110 is an adaptor protein that modulates changes in actin filament integrity. Oncogene. 2001b; 20:6435–6447. [PubMed: 11607843]

Braak E, Arai K, Braak H. Cerebellar involvement in Pick's disease: affliction of mossy fibers, monodendritic brush cells, and dentate projection neurons. Exp Neurol. 1999; 159:153–163. [PubMed: 10486184]

DiNitto JP, Lambright DG. Membrane and juxtamembrane targeting by PH and PTB domains. Biochim Biophys Acta. 2006; 1761:850–867. [PubMed: 16807090]

Dorfleutner A, Cho Y, Vincent D, Cunnick J, Lin H, Weed SA, Stehlik C, Flynn DC. Phosphorylation of AFAP-110 affects podosome lifespan in A7r5 cells. J Cell Sci. 2008; 121:2394–2405. [PubMed: 18577577]

Dorfleutner A, Stehlik C, Zhang J, Gallick GE, Flynn DC. AFAP-110 is required for actin stress fiber formation and cell adhesion in MDA-MB-231 breast cancer cells. J Cell Physiol. 2007; 213:740–749. [PubMed: 17520695]

Fincham VJ, Unlu M, Brunton VG, Pitts JD, Wyke JA, Frame MC. Translocation of Src kinase to the cell periphery is mediated by the actin cytoskeleton under the control of the Rho family of small G proteins. J Cell Biol. 1996; 135:1551–1564. [PubMed: 8978822]

Flynn DC, Leu TH, Reynolds AB, Parsons JT. Identification and sequence analysis of cDNAs encoding a 110-kilodalton actin filament-associated pp60src substrate. Mol Cell Biol. 1993; 13:7892–7900. [PubMed: 8247004]

Frame MC, Brunton VG. Advances in Rho-dependent actin regulation and oncogenic transformation. Curr Opin Genet Dev. 2002; 12:36–43. [PubMed: 11790552]

Fukutani Y, Cairns NJ, Everall IP, Chadwick A, Isaki K, Lantos PL. Cerebellar dentate nucleus in Alzheimer's disease with myoclonus. Dement Geriatr Cogn Disord. 1999; 10:81–88. [PubMed: 10026380]

Gatesman A, Walker VG, Baisden JM, Weed SA, Flynn DC. Protein kinase Calpha activates c-Src and induces podosome formation via AFAP-110. Mol Cell Biol. 2004; 24:7578–7597. [PubMed: 15314167]

Guappone AC, Flynn DC. The integrity of the SH3 binding motif of AFAP-110 is required to facilitate tyrosine phosphorylation by, and stable complex formation with, Src. Mol Cell Biochem. 1997; 175:243–252. [PubMed: 9350057]

Guappone AC, Weimer T, Flynn DC. Formation of a stable src-AFAP-110 complex through either an amino-terminal or a carboxy-terminal SH2-binding motif. Mol Carcinog. 1998; 22:110–119. [PubMed: 9655255]

Hai CM, Hahne P, Harrington EO, Gimona M. Conventional protein kinase C mediates phorbol-dibutyrate-induced cytoskeletal remodeling in a7r5 smooth muscle cells. Exp Cell Res. 2002; 280:64–74. [PubMed: 12372340]

Hering H, Sheng M. Activity-dependent redistribution and essential role of cortactin in dendritic spine morphogenesis. J Neurosci. 2003; 23:11759–11769. [PubMed: 14684878]

Kouzarides T, Ziff E. The role of the leucine zipper in the fos-jun interaction. Nature. 1988; 336:646–651. [PubMed: 2974122]

Larkin MA, Blackshields G, Brown NP, Chenna R, McGettigan PA, McWilliam H, Valentin F, Wallace IM, Wilm A, Lopez R, et al. Clustal W and Clustal X version 2.0. Bioinformatics. 2007; 23:2947–2948. [PubMed: 17846036]

Linder S. Invadosomes at a glance. J Cell Sci. 2009; 122:3009–3013. [PubMed: 19692587]

Linder S, Kopp P. Podosomes at a glance. J Cell Sci. 2005; 118:2079–2082. [PubMed: 15890982]

Lodyga M, De Falco V, Bai XH, Kapus A, Melillo RM, Santoro M, Liu M. XB130, a tissue-specific adaptor protein that couples the RET/PTC oncogenic kinase to PI 3-kinase pathway. Oncogene. 2009; 28:937–949. [PubMed: 19060924]

Lotspeich LJ, Ciaranello RD. The neurobiology and genetics of infantile autism. Int Rev Neurobiol. 1993; 35:87–129. [PubMed: 8463065]

Mayer BJ. SH3 domains: complexity in moderation. J Cell Sci. 2001; 114:1253–1263. [PubMed: 11256992]

Proszynski TJ, Gingras J, Valdez G, Krzewski K, Sanes JR. Podosomes are present in a postsynaptic apparatus and participate in its maturation. Proc Natl Acad Sci U S A. 2009; 106:18373–18378. [PubMed: 19822767]

Qian Y, Baisden JM, Cherezova L, Summy JM, Guappone-Koay A, Shi X, Mast T, Pustula J, Zot HG, Mazloum N, et al. PC phosphorylation increases the ability of AFAP-110 to cross-link actin filaments. Mol Biol Cell. 2002; 13:2311–2322. [PubMed: 12134071]

Qian Y, Baisden JM, Westin EH, Guappone AC, Koay TC, Flynn DC. Src can regulate carboxy terminal interactions with AFAP-110, which influence self-association, cell localization and actin filament integrity. Oncogene. 1998; 16:2185–2195. [PubMed: 9619827]

Qian Y, Baisden JM, Zot HG, Van Winkle WB, Flynn DC. The carboxy terminus of AFAP-110 modulates direct interactions with actin filaments and regulates its ability to alter actin filament integrity and induce lamellipodia formation. Exp Cell Res. 2000; 255:102–113. [PubMed: 10666339]

Qian Y, Gatesman AS, Baisden JM, Zot HG, Cherezova L, Qazi I, Mazloum N, Lee MY, Guappone-Koay A, Flynn DC. Analysis of the role of the leucine zipper motif in regulating the ability of AFAP-110 to alter actin filament integrity. J Cell Biochem. 2004; 91:602–620. [PubMed: 14755689]

Saltel F, Daubon T, Juin A, Ganuza IE, Veillat V, Genot E. Invadosomes: Intriguing structures with promise. Eur J Cell Biol. 2010

Sherwood, L. Human Physiology: From Cells to Systems. 5. Brooks Cole; Kentucky: 2003.

Songyang Z, Shoelson SE, Chaudhuri M, Gish G, Pawson T, Haser WG, King F, Roberts T, Ratnofsky S, Lechleider RJ, et al. SH2 domains recognize specific phosphopeptide sequences. Cell. 1993; 72:767–778. [PubMed: 7680959]

Sparks AB, Rider JE, Hoffman NG, Fowlkes DM, Quillam LA, Kay BK. Distinct ligand preferences of Src homology 3 domains from Src, Yes, Abl, Cortactin, p53bp2, PLCgamma, Crk, and Grb2. Proc Natl Acad Sci U S A. 1996; 93:1540–1544. [PubMed: 8643668]

Squire, LBD.; Bloom, F.; Du Lac, S.; Ghosh, A.; Spitzer, N. Fundamental Neuroscience. 3. Elsevier, Inc; Massachusettes: 2008.

Walker VG, Ammer A, Cao Z, Clump AC, Jiang BH, Kelley LC, Weed SA, Zot H, Flynn DC. PI3K activation is required for PMA-directed activation of cSrc by AFAP-110. Am J Physiol Cell Physiol. 2007; 293:C119–132. [PubMed: 17360811]

Widmaier, ERH.; Strang, K. Vander, Sherman, Luciano's Human Physiology: The Mechanisms of Body Function. 9. McGraw-Hill; New York: 2003.

Xu J, Bai XH, Lodyga M, Han B, Xiao H, Keshavjee S, Hu J, Zhang H, Yang BB, Liu M. XB130, a novel adaptor protein for signal transduction. J Biol Chem. 2007; 282:16401–16412. [PubMed: 17412687]

Yilmaz M, Christofori G. EMT, the cytoskeleton, and cancer cell invasion. Cancer Metastasis Rev. 2009; 28:15–33. [PubMed: 19169796]

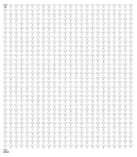

Figure 1. AFAP1L1 sequence

AFAP1L1 coding sequence was divided into codons with corresponding amino acid sequence. Start and stop codons are indicated in bold type.

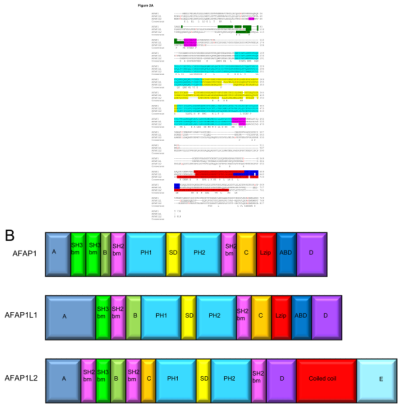

Figure 2. AFAP family members share both sequence and domain similarity

A. AFAP1, AFAP1L1 and AFAP1L2 amino acid sequences were compared using ClustalW2 alignment (Larkin et al., 2007). Consensus sequence between all three family members is labeled as consensus. Intron/exon boundaries are marked by red letters. Predicted SH3 binding motifs are highlighted in green, predicted SH2 binding motifs in pink, predicted PH domains in light blue, predicted Substrate Domain (SD) in yellow, predicted leucine zipper (AFAP1, AFAP1L1) and coiled coil (AFAP1L2) in red and predicted actin binding domain in dark blue. The AFAP1L1 peptide sequence used to create 1L1-CT antibody is underlined.

B. Modular domain organization of AFAP family members was compared. SH3bm = SH3 binding motif, SH2bm = SH2 binding motif, PH1 = pleckstrin homology domain 1, PH2 = pleckstrin homology domain 2, SD = serine/threonine rich substrate domain, Lzip = leucine zipper, ABD = actin binding domain. Sequences that do not correlate with an identified type of modular domain or motif are labeled “A, B, C, D or E”.

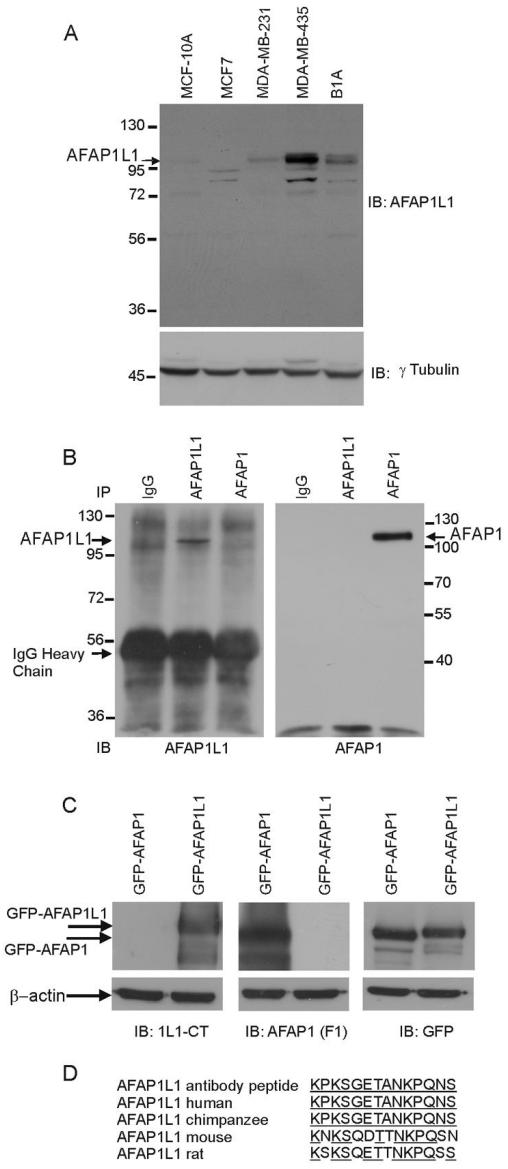

Figure 3. A novel antibody specifically recognizes AFAP1L1

A. Cell lines were lysed in 2X SDS buffer, resolved by 8% SDS-PAGE and transferred to PVDF. The Sigma antibody Ab2 specifically recognized a protein band of 115 kDa. Bands identified as AFAP1L1 and recognized by the Ab2 antibody (top panel) are indicated by an arrow. Gamma tubulin was used as a loading control. Not shown, but in an adjacent lane, was a lysate prepared from 293T cells transfected with untagged AFAP1L1 which was used in identifying the band corresponding to AFAP1L1.

B. Endogenous AFAP1L1 and AFAP1 were specifically immunoprecipitated from Cos-1 cells using 5μg 1L1-CT and F1 polyclonal antibodies respectively and the resolved proteins detected with 1L1-CT (left panel) or AFAP1 monoclonal antibodies (BD Transduction, right panel). Rabbit IgG antibody was used as a control. Note the differences in the molecular weight markers for each western.

C. GFP-AFAP1L1 and GFP-AFAP1 were overexpressed in Cos-1 cells and lysed in 2X SDS buffer. Lysates were resolved by 8% SDS-PAGE, transferred to PVDF membrane and

immunoblotted with either AFAP1L1 (1L1-CT) or AFAP1 (F1) antibody. GFP (top right western) and β-actin (bottom westerns) were used as loading controls.
D. The peptide sequence used to create antibody 1L1-CT was compared to analogous sequences in human, chimpanzee, mouse and rat to show similarity between antibody binding sites.

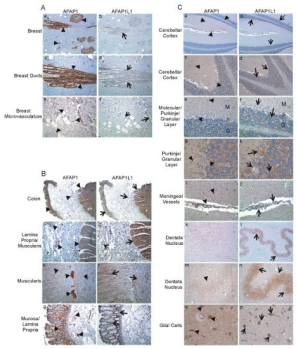

Figure 4. Immunohistochemical analysis of AFAP1L1 shows differential expression from AFAP1 in human tissue

Paraffin-embedded human breast (**A**), colon (**B**) and brain (**C**) tissues were analyzed for AFAP1 and AFAP1L1 localization using F1 and 1L1-CT antibodies respectively. Breast regions include breast ducts (4A panels a–d), breast lobules (4A panels a,b) and microvasculature (4A panels e,f). Colon regions include the mucosa (4B panels a,b,g,h), lamina propria (4B panels a–d, g,h) and muscularis (4B panels a–f). Brain regions include the cerebellar cortex (4C panels a–j), dentate nucleus (4C panels k–n) and glial cells (4C panels o,p). AFAP1L1 is designated by long thin arrows while AFAP1 is designated by arrowheads.

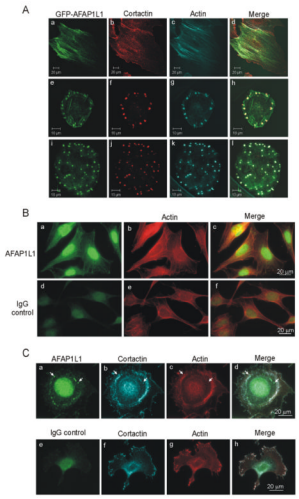

Figure 5. Subcellular localization of GFP-AFAP1L1 shows association with actin and invadosomes

A. A7r5 cells transiently expressing GFP-AFAP1L1 were plated onto fibronectin-coated coverslips and immunolabeled for cortactin (Millipore). Actin was visualized with TRITC-phalloidin (Sigma). Representative images of cells with well-formed stress fibers or podosome formation are shown.

B. MDA-MB-435 cells were plated on fibronectin coated coverslips and immunolabeled for endogenous AFAP1L1 (Sigma Ab2, panel a–c). Rabbit IgG was used as a control (panel d–f) and actin was visualized with AlexaFluor labeled phalloidin. Epifluorescence images of representative cells are shown.

C. MDA-MB-435 cells were transfected with Src 527F construct, plated onto fibronectin coated coverslips and immunolabeled for AFAP1L1 (Sigma Ab1, panel a–d). Rabbit IgG was used as control antisera for AFAP1L1 antibody (panel e–h). Cortactin was immunolabeled with monoclonal anti-cortactin antibodies (4F11, Millipore) and actin was visualized by AlexaFluor labeled phalloidin (panel c, g). Examples of AFAP1L1 co-localizing to invadopodia, actin and cortactin rich punctate structures are marked with white arrows.

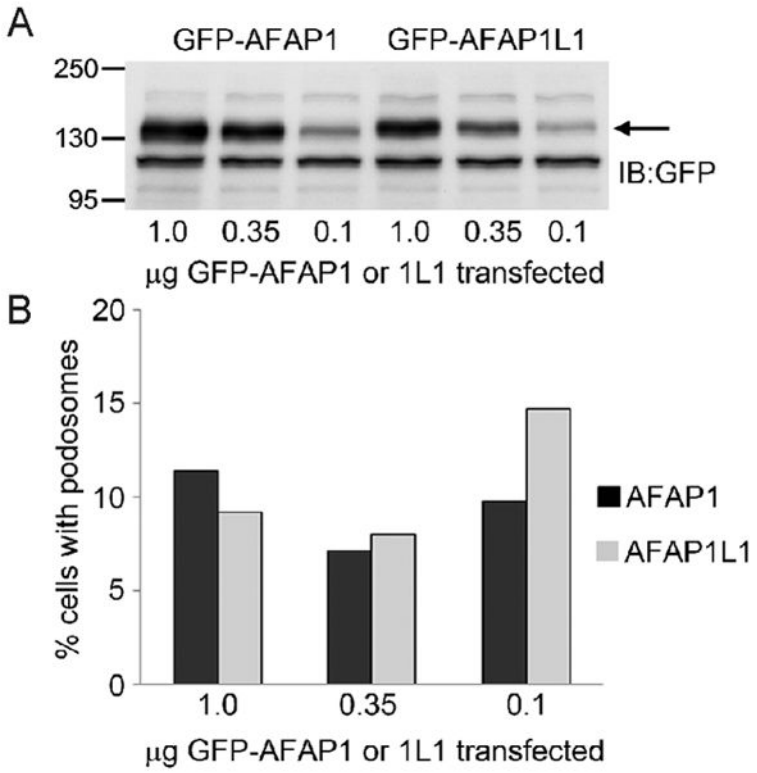

Figure 6. Podosome formation in A7r5 transfected with GFP-AFAP1 or GFP-AFAP1L1 plasmids

A7r5 cells were transfected with the indicated amounts of plasmids encoding either GFP-AFAP1 or GFP-AFAP1L1 (in combination with pcDNA3.1) to bring the total amount of plasmid DNA to 1 µg for each transfection. Twenty four hours post-transfection, the cells were transferred to fibronectin-coated coverslips. Forty-eight hours after transfection, cells were processed for immunofluorescence analysis or used to prepare whole cell SDS lysates. (A) Equal amounts of SDS lysates were resolved by 8% SDS-PAGE and then transferred to PVDF membranes and subsequently probed with an antiserum that recognizes GFP. (B) Cells expressing GFP-AFAP1 or GFP-AFAP1L1 were assessed for podosome formation and the percentage of cells exhibiting podosomes for each transfection was calculated. 150 to 300 cells were counted for each transfection. Panel A and B represents one experiment out of two independently performed experiments.

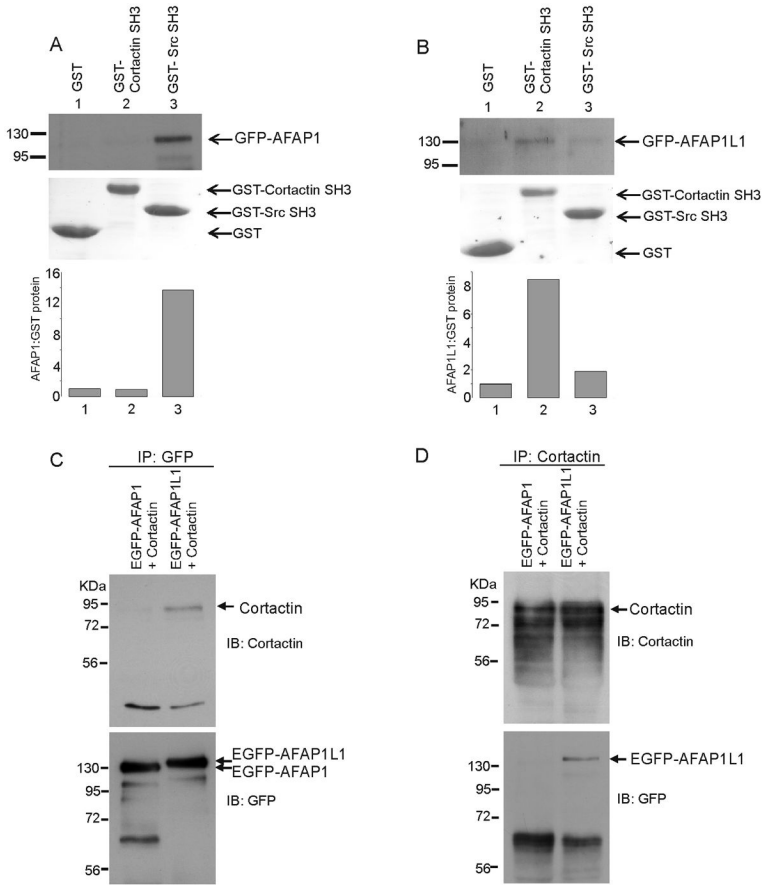

Figure 7. AFAP1L1 interacts with cortactin SH3 domain

A. 1 mg of lysate from 293T cells transiently expressing GFP-AFAP1 was incubated with 50 μg of GST, GST-Src-SH3 domain or GST-cortactin-SH3 domain bound fusion protein to glutathione Sepharose 4B beads and probed for GFP through western blot analysis (upper panel). The lower panel represents a GelCode Blue Stain (ThermoScientific) of GST or GST fusion protein. A graph representing the ratio of AFAP1 pulled down by each GST fusion protein compared to GST control using scanning densitometry is shown.

B. 1mg of lysate from 293T cells transiently expressing GFP-AFAP1L1 was incubated with 50μg of GST, GST-Src-SH3 domain or GST-cortactin-SH3 domain bound to glutathione Sepharose 4B beads and probed for GFP through western blot analysis (upper panel). The lower panel represents a GelCode Blue Stain (ThermoScientific) of GST or GST fusion protein. A graph representing the ratio of AFAP1L1 pulled down by each GST fusion protein compared to GST control using scanning densitometry is shown.

C. 293T transiently expressing cortactin with either GFP-AFAP1 or GFP-AFAP1L1 were immunoprecipitated with anti-GFP antibody, probed for cortactin through western blot analysis (upper panel) and then re-probed for GFP tagged proteins (lower panel).

D. 293T transiently expressing cortactin with either GFP-AFAP1 or GFP-AFAP1L1 were immunoprecipitated with anti-cortactin antibody, probed for GFP tagged proteins through western blot analysis (upper panel) and then re-probed for cortactin (lower panel).

Table 1
AFAP1 and AFAP1L1 immunohistochemical signal intensity in human tissue

The intensity of AFAP1 staining in human breast, colon and brain tissues was analyzed. Staining in breast ducts was scored as ++++ for highest level of intensity. Staining in the dentate nucleus was scored as – for no level of staining. Other tissues labeled for AFAP1 were compared using this scale. AFAP1L1 staining intensity was analyzed in a similar manner, designating AFAP1L1 staining in the dentate nucleus as ++++ and lamina propria as – for no level of staining. Other tissues labeled for AFAP1L1 were compared using this scale.

	AFAP1	AFAP1L1
Breast Lobule	++++	+
Breast Duct	++++	+
Breast Microvasculature	+++	+
Colon Muscularis	++	+++
Colon Mucosa	+++	+++
Colon Lamina Propria	-	-
Cerebellar Cortex	+	+
Cerebellar Granule Cell Layer	++	++++
Cerebellar Purkinje Layer	+	++++
Meningeal Vessels	++++	+
Dentate Nucleus	-	++++
Glial Cells	++	+++